International Journal of Remote Sensing
Vol. 31, No. 14, 20 July 2010, 3799–3819

Development and evaluation of an actual evapotranspiration estimation algorithm using satellite remote sensing and meteorological observational network in Oklahoma

SADIQ IBRAHIM KHAN†‡, YANG HONG*†‡, BAXTER VIEUX†‡ and WENJUAN LIU§

†School of Civil Engineering and Environmental Sciences, University of Oklahoma, Norman, OK 73019, USA

‡Center for Natural Hazard and Disaster Study, Suite 3630, National Weather Center, Norman, OK 73072, USA

§College of Resource and Environment, Northwest A&F University, Yangling, Shaanxi Province, 712100, China

Actual evapotranspiration (AET) estimation using satellite sensors can improve water resources planning and water regulation in irrigated areas. This paper evaluates an AET estimation algorithm developed by integrating satellite remote sensing and an environmental monitoring network in Oklahoma, USA for operational daily water management purpose. First, a surface energy balance evapotranspiration (ET) algorithm is implemented to estimate actual ET by integrating the twice-daily overpass of Moderate Resolution Imaging Spectroradiometer (MODIS) sensor data and Oklahoma's world-class environmental monitoring network—Mesonet—with 5-minute data acquisition in real time. Second, accuracy of the estimated ET is evaluated at the site scale using Ameriflux tower latent heat flux and Mesonet site crop ET on daily, 8-day and seasonal basis. The results showed that MODIS/Mesonet-AET (MM-AET) estimation showed agreement with ground observations, with daily ET bias less than 15% and seasonal bias less than 8%. Additionally, actual ET modelled from a water balance budget analysis in a heavily instrumented basin compares favourably (bias $< 3\%$) with the MM-AET at catchment scales with an order of several hundreds square kilometres. This study demonstrates that (1) the MM-AET estimation is acceptable for daily actual ET estimation and (2) it is feasible to implement the proposed MM-AET algorithm in real time for irrigational water resources management at the scale of irrigation projects in Oklahoma.

1. Introduction

Evapotranspiration (ET) is among the most important processes in the hydrologic cycle and is considered a critical component in diverse disciplines such as those involved in water resource management, agriculture, ecology and climate science. Estimation of spatially distributed ET from agricultural areas is important as irrigation consumes the largest share of water use (Shiklomanov 1998, Glenn *et al.* 2007). Particularly in arid and semi arid biomes, around 90% or more of the annual precipitation can evapotranspired, and thus ET determines the freshwater recharge and discharge from aquifers in these environments (Huxman *et al.* 2005). Moreover, it is projected that climate change will influence the global water cycle and intensify ET

*Corresponding author. Email: yanghong@ou.edu

International Journal of Remote Sensing
ISSN 0143-1161 print/ISSN 1366-5901 online © 2010 Taylor & Francis
http://www.tandf.co.uk/journals
DOI: 10.1080/01431161.2010.483487

globally (Huntington 2006, Meehl *et al.* 2007), consequently impacting the scarce water resources.

Similarly, reliable ET estimates are crucial for efficient use of water resources, especially in agricultural areas for water management (Bouwer *et al.* 2007, Gowda *et al.* 2008). Meanwhile, methods of ET estimation provide potential or reference ET and sometimes crop ET as a product of weather-based reference ET and crop coefficient (K_c) at points, rather than spatiotemporal information about actual ET (Allen *et al.* 2005, Irmak and Irmak 2008). In order to estimate the spatial distribution of ET, a network of 'point' data have to be interpolated to a regional scale.

As an alternative, satellite remote sensing for ET estimation has become a pragmatic approach, with the availability of large amounts of remote sensing data and development of various modelling techniques. Because remotely sensed data have the advantage of large area coverage, frequent updates and consistent quality, remote sensing-based ET estimation has been a subject of many studies (Jackson 1986, Kuittinen 1992, Kite and Pietroniro 1996, Rango and Shalaby 1998, Stewart *et al.* 1999, Mu *et al.* 2007, Sobrino *et al.* 2007, Santanello *et al.* 2007, Wang *et al.* 2007). Although several recent ET models only use remote sensing data for ET estimation (Nishida *et al.* 2003, Norman *et al.* 2003, Jiang *et al.* 2004), integrating meteorological field observations and remote sensing data with optimum spatial and temporal resolution can overcome many of the shortcomings associated with the low spatial coverage of field scale models and the low temporal resolution of satellite data products. Cost effectiveness and easy implementation can be an added advantage. Thus, over the years various ET models have been developed that use remote sensing and ancillary surface and ground-based observations (Seguin 1994, Jiang and Islam 2001, Senay *et al.* 2007). The Surface Energy Balance Algorithm for Land (SEBAL) was described in Bastiaanssen *et al.* (1998, 2005); later the ET estimation model METRIC (Mapping EvapoTranspiration with high Resolution and Internalized Calibration) was developed and applied by the University of Idaho, USA (Allen *et al.* 2007). Some recent studies provide a comprehensive revision of several ET estimation methods. Kalma *et al* (2008) explained different methods for the estimation of ET focusing on remotely sensed surface temperatures, and listed the uncertainties associated with those estimation techniques in terms of limitations of thermal imagery, evaluation criteria of these approaches, and spatial and temporal issues. A recent study by Zhao *et al* (2005) reviewed remote sensing based ET models at regional scale and found that more robust approaches are need to deal with issues related to the current ET models. Some of the problems related to these regional models that need future attention are satellite data retrieval accuracy and physical interpretation of different surface variables, parameterization of land surface fluxes at regional scale, validation of the latent heat flux obtained from models, acquisition of near-surface meteorological data over different spatial resolutions.

Remote sensing ET estimation models have been developed and applied in western USA and many other parts of the world (Allen *et al.* 2007). However, most previous applications have been retrospective in nature (Tang *et al.* 2009), in part because of the lack of timely availability of satellite images with relatively frequent revisits, e.g. Landsat 16-day. Furthermore, many ground *in situ* observations do not provide data in real time. As a result, although the retrospective ET estimates can be useful in modelling studies, they cannot aid operational water management decision-making in real time.

With the availability of twice-daily MODIS products and well-distributed world-class environmental monitoring stations from Mesonet (http://mesonet.org) with 5-minute acquisition frequency, Oklahoma provides a unique setting to develop and apply a real-time ET estimation algorithm for timely water use and irrigation management. In past decades the primary method for estimating ET relied on site-based weather station measurements, which are inadequate to monitor the spatial variability of ET over large regions and only focus on potential rather than actual ET. Therefore, the main objective of this study is to assess the potential of satellite remote sensing products to implement an operational ET algorithm for estimating daily actual ET on a large scale in Oklahoma. Specifically, the objectives of this research are: (1) to estimate the actual evapotranspiration (AET) by integrating MODIS daily products and the Oklahoma Mesonet observational network with 5-minute data acquisition through a simplified surface energy balance approach, METRIC (i.e. MOD/METRIC; hereinafter MM-AET); (2) to evaluate the robustness of the MM-AET approach using site-based flux tower observations and basin-scale water balance modelling results; and (3) to assess the feasibility of implementing MM-AET for an operational AET estimation algorithm appropriate for regional scales, e.g. the scale of irrigation projects, rather than individual fields, in real-time.

Subsequent applications in ET estimation have opened frontiers in agricultural water use and groundwater resources management at different scales and diverse landscapes. ET estimation by integrating remote sensing data and meteorological field observations with optimum spatial and temporal resolution can overcome many of the shortcomings associated with low spatial coverage of field scale models. Cost effectiveness and easy implementation of spatially distributed ET estimation for water management are added advantages.

2. Study area and data

2.1 *Study area*

Oklahoma provides a unique setting to implement and evaluate remote sensing ET estimation methods. The region has an extensive and well distributed meteorological observation network, known as Mesonet stations (figure 1(*a*)). In addition to Mesonet towers, there are a fair number of surface flux observation stations (AmeriFlux towers) in the Southern Great Plain (SGP), the first field measurement site established by USA Department of Energy's Atmospheric Radiation Measurement (ARM) program. AmeriFlux, part of the global Fluxnet network that was established in 1996 provide continuous observations of ecosystem level exchange of CO_2, water, energy and other climatological variables (Baldocchi *et al.* (2001); http://www.daac.ornl.gov/FLUXNET/fluxnet.html). Moreover, Oklahoma has several heavily instrumented watersheds, which enable us to compare the remote sensing actual ET estimates with ET obtained from water balance models at the catchment scale. The Blue River Basin is located in south central Oklahoma, covering an approximate area of 1200 km^2. The upper part of the basin overlies the Arbuckle-Simpson aquifer, which provides water to streams and rivers as baseflow, constituting the principal water source of many towns in the Chickasaw National Recreation area, including Ada and Sulphur, where the water is used for public water supply, irrigation, recreation, agriculture, industrial use and mining. A map showing the study area, with AmeriFlux towers, Mesonet sites and Blue River Basin characteristics is

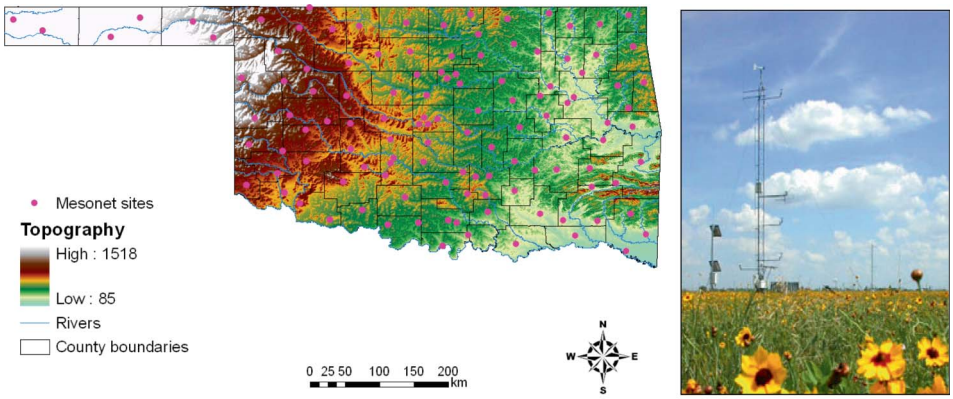

(*a*)

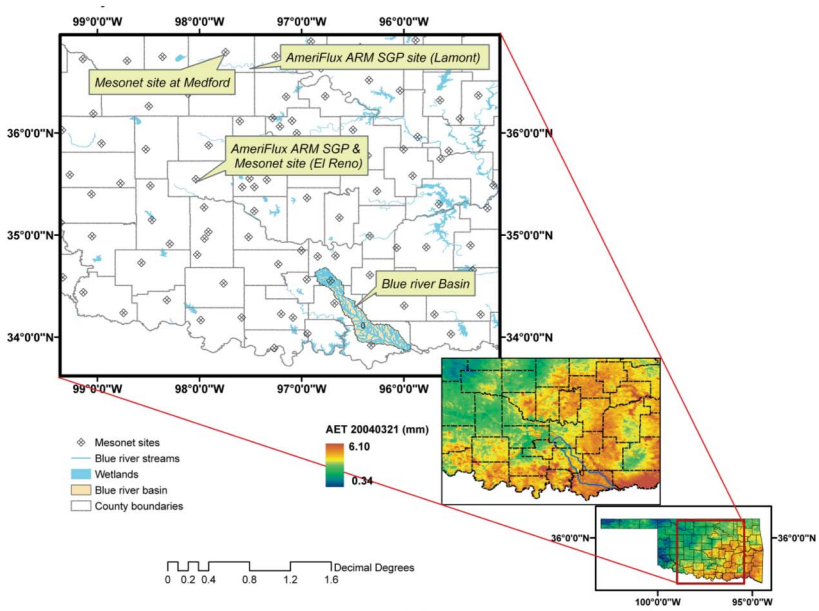

(*b*)

Figure 1. (*a*) Mesonet site locations (pink dots). On the right is the 10-m tall monitoring tower and instrumentations. (*b*) Study area with Ameriflux towers, Mesonet sites and Blue River Basin.

shown in figure 1(b). The study area extends over the state of Oklahoma with longitude from 94.4° W to 103.0° W and latitude from 33.6° N to 37.0° N.

2.2 *Oklahoma meteorological observations*

The Oklahoma Mesonet is a world-class network of environmental monitoring stations jointly managed by the University of Oklahoma (OU) and Oklahoma State University (OSU). Established as a multipurpose network, it operates more

than 120 automated surface observing stations covering the state of the Oklahoma and has measured comprehensive meteorological, hydrological and agricultural variables since the early 1990s (McPherson *et al.* 2007). Mesonet stations have collected over 3 758 558 640 observations since 1 January 1994. At each site, the environment is measured by a set of instruments located on or near a 10-m-tall tower. The measurements are packaged into 'observations' every 5 minutes; then the observations are transmitted to a central facility every 5 minutes, 24 hours per day year-round (http://www.mesonet.org). The Oklahoma Climatological Survey (OCS) at OU receives the observations, verifies the quality of the data and provides the data to Mesonet customers. It only takes 5–10 minutes from the time the measurements are acquired until they become available to the public. In this study we used reference ET calculated by the Oklahoma Mesonet. The climatological variables that Mesonet uses in their reference ET model are solar radiation (W m^{-2}), wind speed at 2 m (m s^{-1}), air temperature at 1.5 m (°C), relative humidity at 1.5 m (%) and station pressure (kPa). Mesonet reference ET calculation is explained under the model description in §3.2.

2.3 *Satellite remote sensing data*

The Moderate Resolution Imaging Spectroradiometer (MODIS) sensors, with 36 spectral bands (20 reflective solar and 16 thermal emissive bands), provide unprecedented information regarding vegetation and surface energy (Justice *et al.* 2002), which can be used to develop a remotely sensed ET model (Mu *et al.* 2007). ET-relevant MODIS data used in this study are listed in table 1. Wan and Li (1997) described the retrieval of MOD11 land surface temperature (LST) and emissivity from MODIS data. For detailed information about MOD09

Table 1. ET-relevant NASA MODIS data products.

Product ID	Layer	Spatiotemporal resolution	MODIS QA-SDS[a] analysis (quality flags passed)
MOD11A2	Land surface temperature (LST)	1 km[b], overpass	General quality: good
	Emissivity view angle[c]	1 km, overpass	
	Recording time	1 km, overpass	
		1 km, overpass	
MOD13Q1	Vegetation index NDVI	1 km, 16-day	Quality: good–perfect Mixed clouds: no
MOD43B3	Albedo	1 km, 16-day	Quality: good and acceptable Snow: no
MOD09Q1	Red reflectance NIR reflectance	250 m, 8-day	Quality: good Clouds: clear Band quality: highest
MOD15A2	Leaf Area Index (LAI)	1 km, 8-day	Quality: good Cloud: clear or assumed clear
MOD12Q1	Land cover type	250 m, annual	Quality: good

[a]Quality assessment science datasets.
[b]The swath products were gridded using the MODIS reprojection tool (MRT).
[c]The view angles were analysed to remove effects from scan geometry caused by increasing Instantaneous Field of View (IFOV) towards the edges of the scan lines.

surface reflectance products see Vermote *et al.* (1997). The algorithm for retrieving the vegetation index (MOD13) is presented by Huete *et al.* (2002). The computation of broadband albedo (MOD43B3) by integrating bi-hemispherical reflectance data modelled over MODIS channels 1–7 (0.3–5.0 um) is explained in Schaaf *et al.* (2002). MODIS provides two black sky and white sky albedo products (Jin *et al.* 2003, Wan *et al.* 2004); we used average of both products. The change in albedo calculation from aerosol optical depth and solar zenith angle are small and assumed to yield insignificant errors in vegetated areas. The missing albedo data can be filled with the method proposed by Zhao *et al.* (2005). All NASA MODIS land products include quality assessment science datasets (QA-SDS), which consider the atmospheric conditions in term of cloud cover and aerosol content, algorithm choices, processing failure and error estimates (Colditz *et al.* 2006). These data products were extracted and processed from the Land Processes Distributed Active Archive Center (LP DAAC) at the U.S. Geological Survey (USGS) EROS Data Center, with the standard hierarchical data format (http://LPDAAC.usgs.gov). For more information on MODIS, please refer to http://modis.gsfc.nasa.gov.

3. MM-AET estimation algorithm

3.1 *Estimation of instantaneous actual ET using a simplified surface energy balance approach*

In this paper we used a simplified version of the surface energy balance (SEB) approach, namely METRIC, to estimate actual ET (AET) while maintaining the major assumptions in the METRIC and SEBAL methods. The central scientific basis of SEB is to compute the ET as the residual of the energy balance equation:

$$\mathrm{LE} = \lambda(\mathrm{ET}) = R_\mathrm{n} - G - H, \tag{1}$$

where λ is the latent heat of water evaporation constant; R_n is net radiation flux; G is soil heat flux; and H is sensible heat flux to the atmosphere (units are W m^{-2}). Thus, ET is calculated as the residual amount of energy remaining from the surface energy balance budget, where the available R_n is shared between the G and the atmospheric convective fluxes (sensible heat H and latent heat LE). The R_n and other components (i.e. G) of SEB can be derived through remote sensing information and surface properties such as albedo, leaf area index, vegetation cover, surface temperature and meteorological observations (Su *et al.* 2002, Bastiaanssen *et al.* 2005, Allen *et al.* 2007). The equation to calculate the net radiation flux is given by

$$R_\mathrm{n} = (1-\alpha)R_\mathrm{swd} + \varepsilon R_\mathrm{lwd} - \varepsilon\sigma T_\mathrm{s}^4, \tag{2}$$

where α is surface albedo; R_swd and R_lwd are incoming shortwave and longwave radiation respectively; ε is surface emissivity; σ is the Stefan–Bolzmann constant, and T_s is the land surface temperature. Soil heat flux (G) was modelled as a function of R_n, vegetation index, surface temperature and surface albedo (Bastiaanssen *et al.* 1998):

$$G = R_\mathrm{n}\left[(T_\mathrm{s} - 275.15)(0.0038 + 0.0074\alpha)\left(1 - 0.98(\mathrm{NDVI})^4\right)\right], \tag{3}$$

where NDVI is the Normalized Difference Vegetation Index [$(R - \mathrm{NIR})/(R + \mathrm{NIR})$]. R is reflectance in the red band and NIR is reflectance in the near-infrared band.

Sensible heat flux (H) is defined by the bulk aerodynamic resistance equation, which uses aerodynamic temperature (T_{aero}) and aerodynamic resistance to heat transfer (r_{ah}):

$$H = \rho_{\mathrm{a}} C_{p_{\mathrm{a}}} (T_{\mathrm{aero}} - T_{\mathrm{a}})/r_{\mathrm{ah}}, \tag{4}$$

where ρ_{a} is air density (kg m^{-3}), C_{p_a} is specific heat of dry air (1004 J kg^{-1} K^{-1}), T_{a} is average air temperature (K), T_{aero} is average aerodynamic temperature (K), and r_{ah} is aerodynamic resistance (s m^{-1}) to heat transport. In SEBAL and METRIC (Allen *et al.* 2005, Tasumi *et al.* 2005), H usually results from dividing the gradient of vertical temperatures (dT) by the aerodynamic resistance of heat transport (r_{ah}), without needing to know T_{a} or T_{aero}.

$$H = \rho_{\mathrm{a}} C_{p\mathrm{a}} \left(\frac{dT}{r_{\mathrm{ah}}} \right). \tag{5}$$

Allen *et al.* (2007) explained that dT is a parameter that represents the near-surface temperature difference between two different elevations z_1 and z_2, and that the indexing of dT to T_{s} does not rely on absolute values of T_{s}, which allegedly reduces the error in calculating H substantially. One key assumption of SEBAL and METRIC is the linear relationship between dT and land surface temperature, T_{s} (Bastiaanssen *et al.* 1998, Allen *et al.* 2005), characterized in equation (6).

$$dT = a + bT_{\mathrm{s}}, \tag{6}$$

where a and b are empirically determined constants.

The determination of a and b in equation (6) involves locating dry or wet limiting cases, a dry-limit pixel with high T_{s} and a wet-limit pixel with low T_{s}. Thus, the linear equation can be computed using the two anchor points. Typically a dry bare soil surface is selected as the 'hot pixel', and latent heat flux $(\mathrm{LE})_{\mathrm{dry}}$ from the pixel is assumed zero, which means that all available energy is partitioned to the sensible heat H_{dry}. Therefore, at the dry limit, the latent heat (or the evaporation) becomes zero due to the limitation of soil moisture, and the sensible heat flux is at its maximum value. Once these pixels have been identified, the energy balance of equation (1) can be solved for

$$(\mathrm{LE})_{\mathrm{dry}} = (R_{\mathrm{n}} - G)_{\mathrm{dry}} - H_{\mathrm{dry}} = 0 \ \mathit{or}\ H_{\mathrm{dry}} = (R_{\mathrm{n}} - G)_{\mathrm{dry}}. \tag{7}$$

For the wet-limit pixel H_{wet} is assumed zero and $(\mathrm{LE})_{\mathrm{wet}}$ is assumed to have an LE value equal to 1.05 times that expected for a tall reference crop (i.e. alfalfa; Allen *et al.* (2007)). Therefore, the energy balance of equation (1) for the wet limit can be solved as:

$$\mathrm{LE}_{\mathrm{wet}} = (R_{\mathrm{n}} - G)_{\mathrm{wet}} - H_{\mathrm{wet}} = (R_{\mathrm{n}} - G)_{\mathrm{wet}} = 1.05(\mathrm{ET})_{\mathrm{r}}, \tag{8}$$

where $(\mathrm{ET})_{\mathrm{r}}$ is standardized reference evapotranspiration (mm d^{-1}for daily or mm h^{-1} for hourly time steps). With the determination of H_{dry} and H_{wet}, proportional coefficients of other pixels can be calibrated within the same remote sensing image using a linear interpolation based on LST between these two extreme pixels. For more detail, please refer to Bastiaanssen *et al.* (1998) and Allen *et al.* (2005). Here we adopted the METRIC approach to identify hot and cold pixels. The landscape is simplified as a mixture of vegetation and bare soil. Fractional canopy coverage f_{c}, whose value is

between 0 and 1, is related to MODIS Normalized Difference Vegetation Index (NDVI):

$$f_c = \frac{(\mathrm{NDVI}) - (\mathrm{NDVI})_{\min}}{(\mathrm{NDVI})_{\max} - (\mathrm{NDVI})_{\min}}. \tag{9}$$

The surface energy balance computation is then based on determination of the relative instantaneous ET fraction ($(\mathrm{ET})_f$) given by:

$$(\mathrm{ET})_f = \frac{\lambda E}{H + \lambda E} = \frac{\dfrac{H_{\mathrm{dry}} - H}{H_{\mathrm{dry}} - H_{\mathrm{wet}}} \lambda E_{\mathrm{wet}}}{R_{\mathrm{n}} - G}. \tag{10}$$

Equations (1)–(10) above constitute the basic formulation of SEB. The actual sensible heat flux H is obtained by solving a set of nonlinear equations and is constrained in the range set by the sensible heat flux at the wet limit H_{wet} and the dry limit H_{dry}. An alternative to compute the $(\mathrm{ET})_f$ is to assume, according to Senay *et al.* (2007), that hot-dry pixels experience lowest ET and cold-wet pixels represent maximum ET throughout the study area. The temperature of hot and cold pixels can be used to calculate proportional fractions of ET on a per pixel basis. Thus, the $(\mathrm{ET})_f$ can also be calculated for each pixel by applying the following equation (equation (11)) to each of the MODIS land surface temperature grids:

$$(\mathrm{ET})_f = \frac{T_{\mathrm{hot}} - T_{i,j}}{T_{\mathrm{hot}} - T_{\mathrm{cold}}}, \tag{11}$$

where T_{hot} is the average of the hot pixels selected for the study domain; T_{cold} is the average of the cold pixels; and $T_{i,j}$ is the MODIS land surface temperature value for any pixel in the composite image.

In practice, $(\mathrm{ET})_f$ is used in conjunction with reference ET ($(\mathrm{ET})_r$) described in §3.2 to calculate the per-pixel instantaneous actual ET ($(\mathrm{ET})_a$) values in a given scene according to METRIC in Allen *et al.* (2005):

$$(\mathrm{ET})_a = (\mathrm{ET})_f \times (\mathrm{ET})_r. \tag{12}$$

A key assumption of this method is that the $(\mathrm{ET})_f$ value is nearly constant, which is often observed to be the case (Shuttleworth *et al.* 1989, Sugita and Brutsaert 1991, Brutsaert and Sugita 1992, Crago 1996). This allows instantaneous estimate of $(\mathrm{ET})_f$ at MODIS overpass times to be extrapolated to estimate daily average ET. The daily ET can thus be determined as:

$$(\mathrm{AET})_{\mathrm{daily}} = \sum_{\mathrm{i}=1}^{\mathrm{day}} ((ET)_f \times (ET)_r^i), \tag{13}$$

where $(\mathrm{AET})_{\mathrm{daily}}$ is the actual ET on a daily basis (mm d^{-1}), and i is temporal resolution of computed reference ET. The $(\mathrm{ET})_r$ is the reference ET used from the Oklahoma Mesonet ET Model explained below.

3.2 *Oklahoma Mesonet reference ET model*

The Oklahoma reference ET calculations are based on the standardized Penman–Monteith reference ET equation recommended by the American

Society of Civil Engineers (ASCE) and the computational procedures found in Allen *et al.* (1994a, 1994b) based on the experimental work in Kimberly, Idaho (Wright 1996):

$$(\mathrm{ET})_{\mathrm{r}} = \frac{0.408(R_{\mathrm{n}} - G) + \gamma \dfrac{C_{\mathrm{n}}}{T + 273} u_2 (e_{\mathrm{s}} - e_{\mathrm{a}})}{\gamma (C_{\mathrm{d}} u_2)}, \tag{14}$$

where $(\mathrm{ET})_{\mathrm{r}}$ = standardized reference evapotranspiration (mm $\mathrm{d}^{-1}$for daily or mm h^{-1} for hourly time steps); R_{n} = calculated net radiation at the crop surface (MJ m^{-2} d^{-1} for daily time steps or MJ m^{-2} h^{-1} for hourly time steps); G = soil heat flux density at the soil surface (MJ m^{-2} d^{-1} for daily time steps or MJ m^{-2} h^{-1} for hourly time steps); T = mean daily or hourly air temperature at 1.5–2.5 m height (°C); u_2 = mean daily or hourly wind speed at 2 m height (m s^{-1}); e_{s} = saturation vapour pressure at 1.5–2.5 m height (kPa), for daily computation, the value being the average of e_{s} at maximum and minimum air temperature; e_{a} = mean actual vapour pressure at 1.5–2.5 m height (kPa); γ = psychrometric constant (kPa $^{\circ}\mathrm{C}^{-1}$); C_{n} = numerator constant that changes with reference type (900 for short grass and 1600 for tall grass) and calculation time step; and C_{d} = denominator constant that changes with reference type (0.34 for short grass and 0.38 for tall grass) and calculation time step.

4. Results and evaluation

We implemented the above mentioned MM-AET estimation algorithm for three years (2004–2006) based on MODIS remote sensing data listed in table 1 and Oklahoma Mesonet observational network shown in figure 1(*a*). For more details of the 5-minute Mesonet weather variables, please refer to http://meso-net.org. In this study MM-AET estimates are evaluated on daily, 8-day and seasonal basis at both field and catchment levels. Two different field sources described below are used to compare the estimated results: one with AmeriFlux towers for latent heat flux observation and the other with Mesonet sites for crop ET. The location and general site characteristics are summarized in figure 1(*b*) and table 2. Table 2 lists the two Atmospheric Radiation Measurements (ARM) SGP eddy covariance tower sites, located at the ARM SGP extended facilities in Lamont and El Reno, Oklahoma, respectively. The two Mesonet sites at El Reno and Medford with Crop ET data are also selected for the comparison.

Table 2. Validation locations of ARM SGP AmeriFlux towers and Mesonet sites.

	Elevation (m)	County	Surface type
ARM SGP site			
El Reno	421	Canadian	Pasture (ungrazed)
Lamont	315	Grant	Pasture and wheat
Mesonet site			
Medford	332	Grant	Wheat and pasture
El Reno	419	Canadian	Pasture

4.1 *Validation at AmeriFlux sites*

The ARM instruments and measurement applications (http://www.arm.gov) are well established and have been used for validating estimates of net primary productivity, evaporation and energy absorption that are being generated by sensors on the National Aeronautics and Space Administration (NASA) TERRA satellite (http://public.ornl.gov/ameriflux/) in many studies (Heilman and Brittin 1989, Halldin and Lindroth 1992, Lewis 1995, Shuttleworth 1991, Venturini *et al.* 2008). The ARM stations are widely distributed over the whole study domain but only two provide the latent flux data for the study time period. Thus, ET estimates were compared with the flux tower observations at Lamont and El-Reno as shown in figures 2 and 3, respectively.

Table 3 provides statistical variability for observed and estimated actual ET for the defined temporal scales. In table 3, the root mean square errors (RMSE), bias ratio,

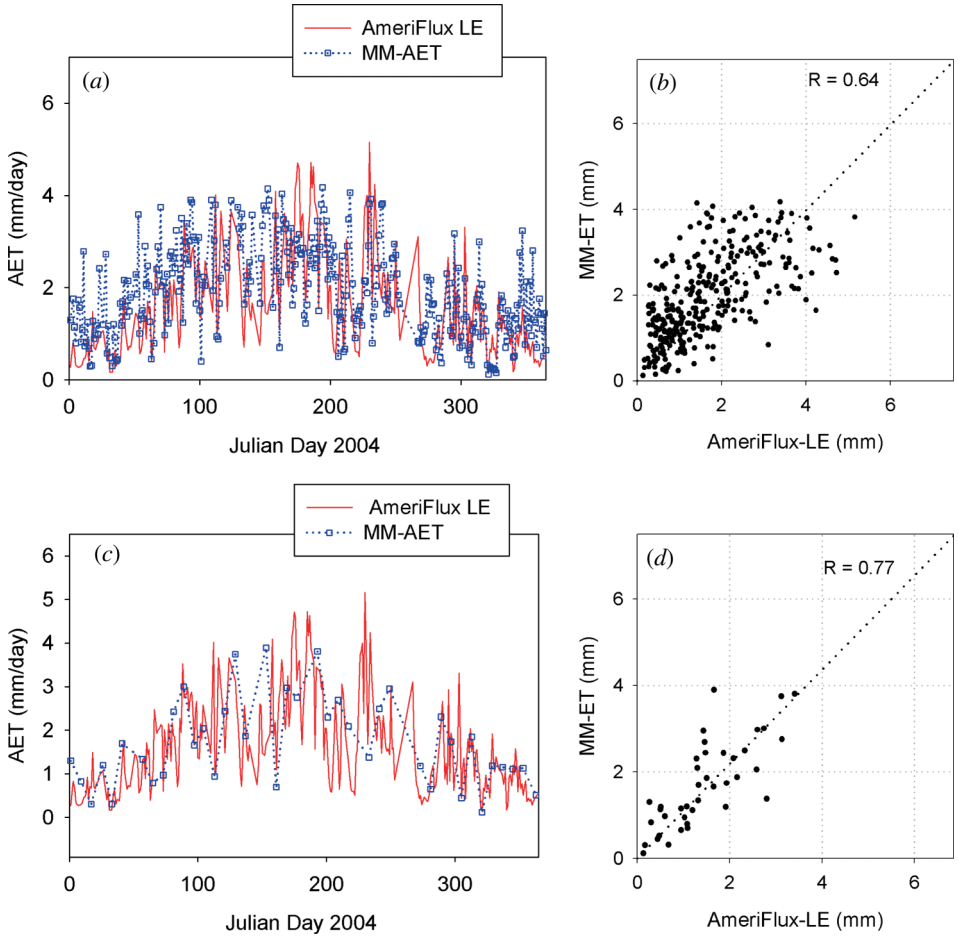

Figure 2. 2004 comparisons of daily and 8-day mean actual ET from AmeriFlux tower observations and the Surface Energy Balance-based MM-AET estimates at ARM SGP Lamont site (when available). Panels (*a*) and (*b*) show the daily time series and scatter plot comparison; (*c*) and (*d*) are for every eighth day.

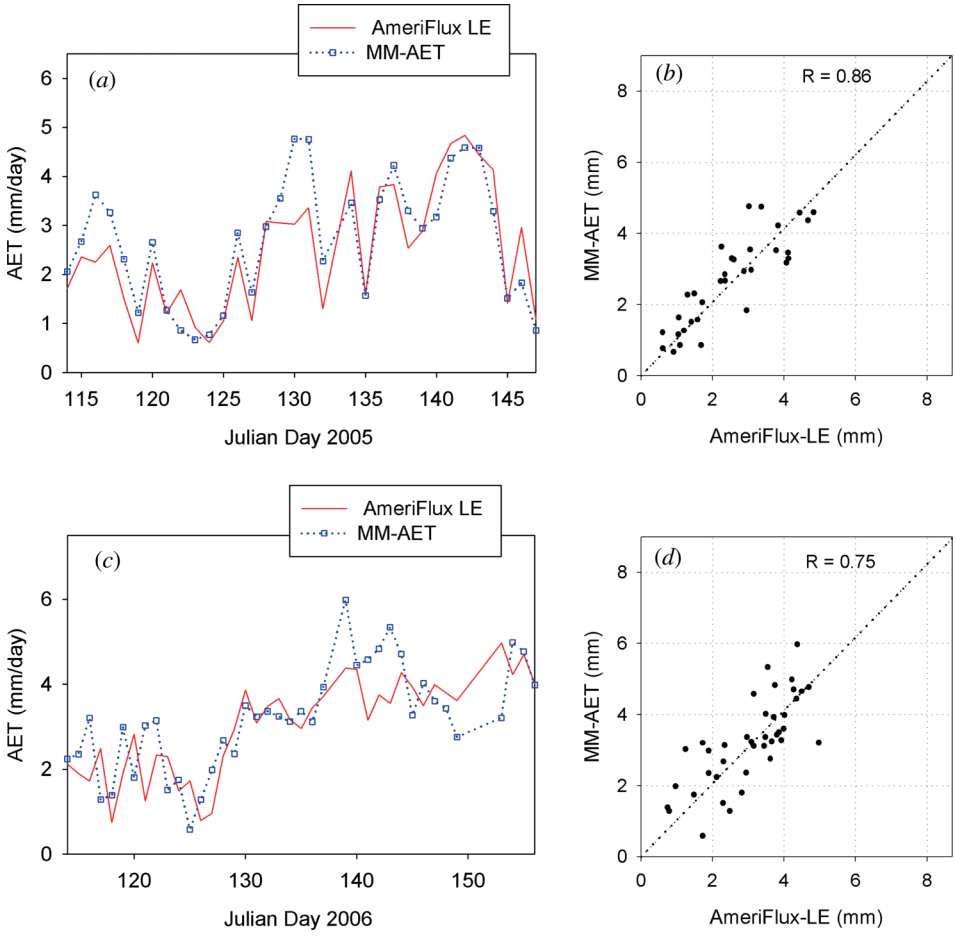

Figure 3. Comparisons of actual ET from AmeriFlux tower observations and SEB-based MM-AET estimates at ARM SGP El-Reno site for growing season. Panels (*a*) and (*b*) show the daily time series and scatter plot comparison for 2005; (*c*) and (*d*) are for 2006.

and correlation coefficients are presented for each day, every eighth day and for summer and fall season. In general, bias ratios are less than 15% of the mean values for daily and 8-day with a correlation of 0.64 and 0.77, respectively. These values indicate the ET estimates correlate relatively well with the measurements. It should be

Table 3. Comparisons of daily and 8-day mean SEB-based MM-AET estimates with AmeriFlux observations at ARM SGP Lamont site for 2004.

	AmeriFlux mean (mm)	SEB mean (mm)	Bias (mm)	% Bias ratio	CC	% RMSE
Daily	1.63	1.87	0.28	15	0.64	56
8-day	1.46	1.70	0.24	13	0.77	46
Summer	2.46	2.62	0.16	6	—	—
Fall	1.70	1.83	0.13	7	—	—

Table 4. Comparisons of daily SEB-based actual ET estimates with AmeriFlux observations at ARM SGP, El-Reno site for 2005.

Days Of Year	AmeriFlux mean (mm)	SEB mean (mm)	Bias (mm)	Bias ratio	CC	% RMSE
24 April 2005–27 May 2005	2.49	2.68	0.19	8	0.86	27
24 April 2006–05 July 2006	3.04	3.22	0.17	6	0.75	28

noted that the daily and 8-day results are impacted by the image quality in terms of cloud cover. Therefore, the daily and 8-day bias and RMSE for those days tend to be larger than the seasonal values. The bias ratios are less than 8% at Lamont site for both summer and fall season.

Table 4 lists the comparison results for another AmeriFlux tower site at El-Reno for growing seasons in 2005 and 2006. Both seasons show relative small bias ratio (7.6% and 5.9%), high correlation (0.86 and 0.75) and low RMSE (27% and 28%).

4.2 *Validation with crop ET at Mesonet sites*

The ET estimates are also evaluated with the crop ET at Grant (Medford site) and Canadian (El-Reno site) counties (figure 1 and table 2) during the wheat growing season in 2004–2006. Figures 4 and 5 plot the daily time series and scatter plots for the sites, respectively. There is a good agreement as the scatter graphs correspond well with the *in situ* crop ET. Table 5 summarizes the comparisons at the Medford and El-Reno sites (figure 6). The bias ratios are around −7% and 3% at the Medford site for 2004 and 2005 respectively. Similarly, the correlation coefficient values indicate ET estimates correlated strongly with values of 0.84 and 0.80 for 2004 and 2005 observations at the Medford site. MM-AET estimates at El-Reno show slightly higher biases but are in general agreement with the measurements. The correlation coefficient values also indicate that the ET estimates correlate relatively well at El-Reno site for 2005 with values of 0.82 and less correlation of 0.51 for 2006. Noise for 2006 can be attributed to the image quality in terms of cloud cover.

4.3 *Validation at Blue River Basin*

In this study the water balance budgeted ET from an earlier study in the Blue River Basin was used to compare the MM-AET. A climatological water budget for the USGS gauging stations was estimated using the following equation:

$$\Delta S = P - G_{\mathrm{w}} - R - ((\mathrm{PET}) - (\mathrm{AET})), \tag{15}$$

where ΔS is the change in storage, P is precipitation, G_{w} is baseflow, R is direct runoff, PET is potential evapotranspiration and AET is actual evapotranspiration. This hydrological budget assumes that there is no significant change in storage from year to year ($\Delta S = 0$), which allows computing actual evapotranspiration, AET, using pan evaporation. Table 6 shows several hydro-meteorological records that were used in the earlier study to conduct water budget analysis for the basin. Pan evaporation observations were incorporated to calculate the ET. Shown in figure 7, monthly comparison between MM-AET and water balance budget ET shows favourable

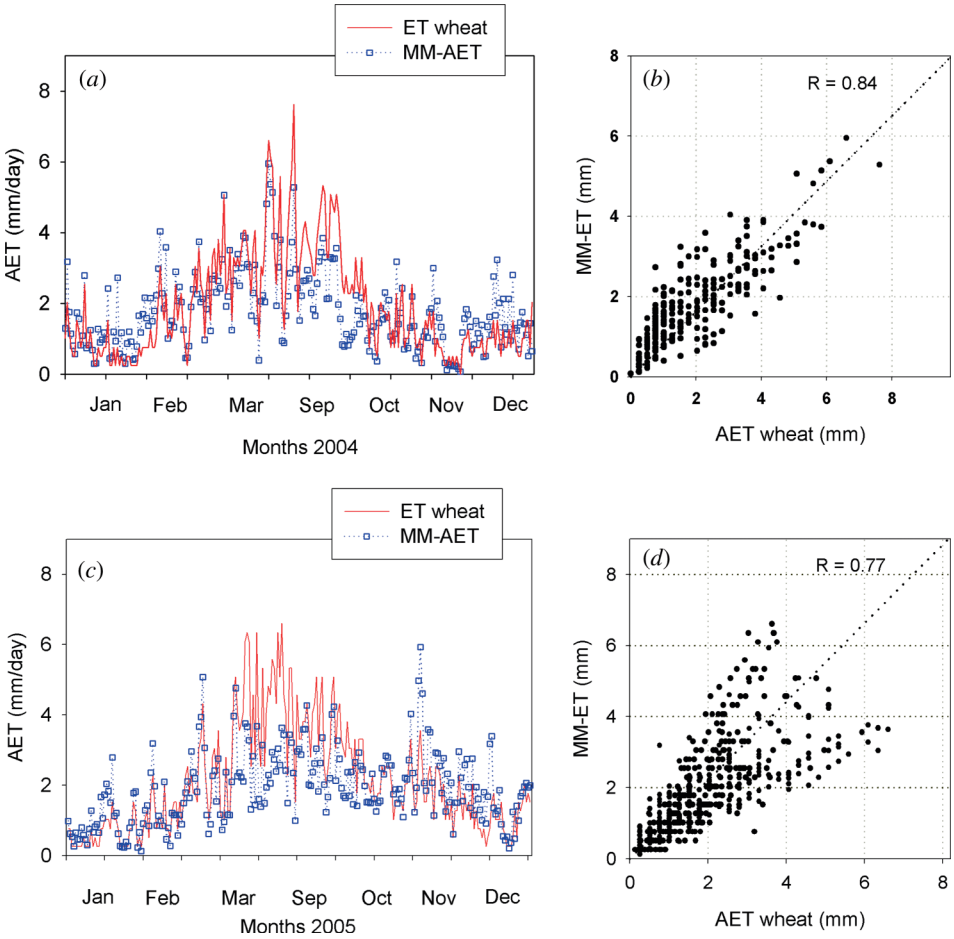

Figure 4. Comparisons of crop ET (wheat) and SEB-based MM-AET estimates at Mesonet Medford site. Panels (*a*) and (*b*) show the 2004 time series and scatter plot; (*c*) and (*d*) are for 2005.

agreement, with bias ratio less than 3%, correlation coefficient 0.68 and RMSE of 31% at catchment scale.

We compared the spatially varied parameters used in the determination of actual ET such as NDVI and spatially averaged actual ET over Blue River Basin for three years. Figure 8 shows seasonal dynamics of NDVI throughout the three-year time series. The vegetation indices started to rapidly rise in early April, reached their peak values in June, and then declined gradually and stayed low after late October or early November; which delineates the length of the plant growing season. This reconfirms the seasonal cycle of ET with vegetation indices in these mixed natural ecosystems and agricultural areas, as shown in previous studies (Choudhury *et al.* 1994, Seevers and Ottomann 1994, Bausch 1995, Szilagyi 2000, 2002, Hunsaker *et al.* 2003, 2005, Houborg and Soegaard 2004, Nagler *et al.* 2005, Senay *et al.* 2007). The existence of a clear spatial and temporal patter in the NDVI–ET relationship may help define biophysical conditions prerequisite for the successful application of vegetation indices in basin-based water-balance modelling (Szilagyi 2002).

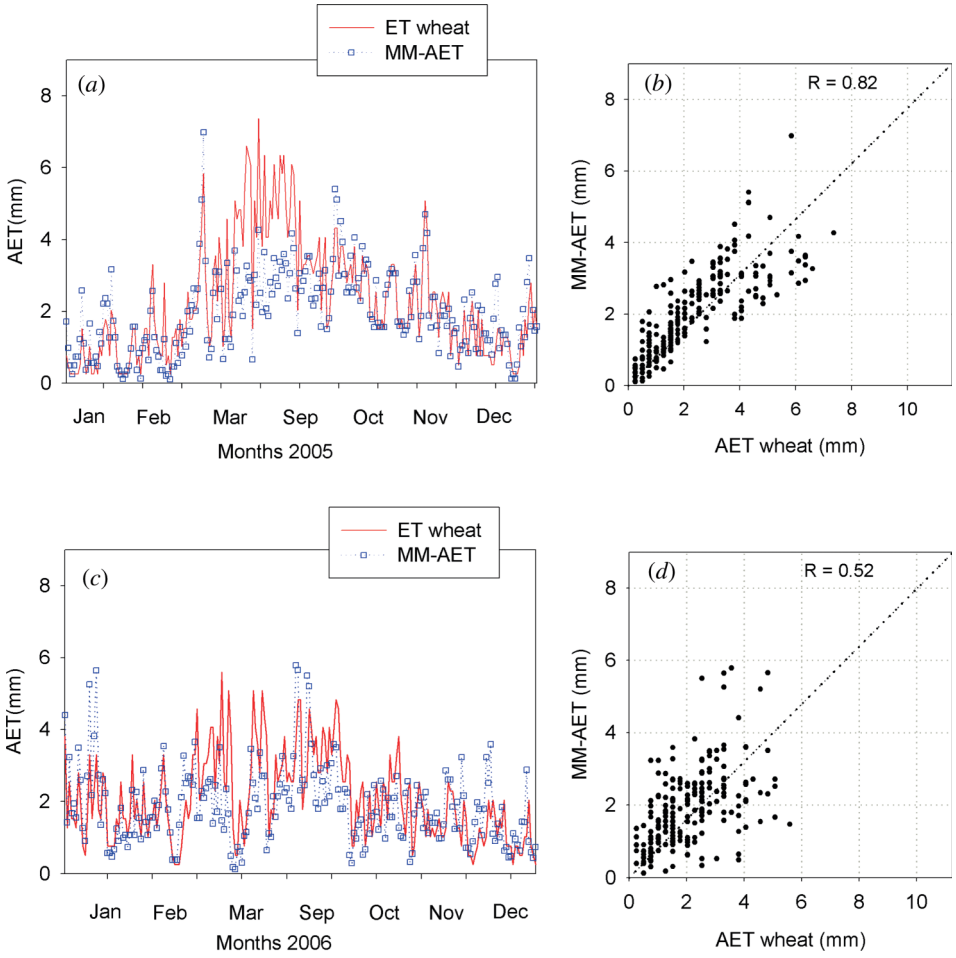

Figure 5. Comparisons of crop ET (wheat) and SEB-based MM-AET estimates at Mesonet El-Reno site. Panels (*a*) and (*b*) show the 2005 time series and scatter plot; (*c*) and (*d*) are for 2006.

Table 5. Comparisons of actual ET estimates with crop ET at Medford and El Reno sites for wheat growing seasons.

	ET wheat crop mean (mm)	SEB mean (mm)	Bias	Bias ratio	CC	% RMSE
Medford site						
2004 wheat crop season	1.91	1.77	–0.14	–7	0.84	42
2005 wheat crop season	1.77	1.83	0.06	4	0.80	41
El-Reno site						
2005 wheat growing season	2.28	1.97	–0.31	–14	0.82	42
2006 wheat growing season	2.06	1.87	–0.19	–9	0.51	54

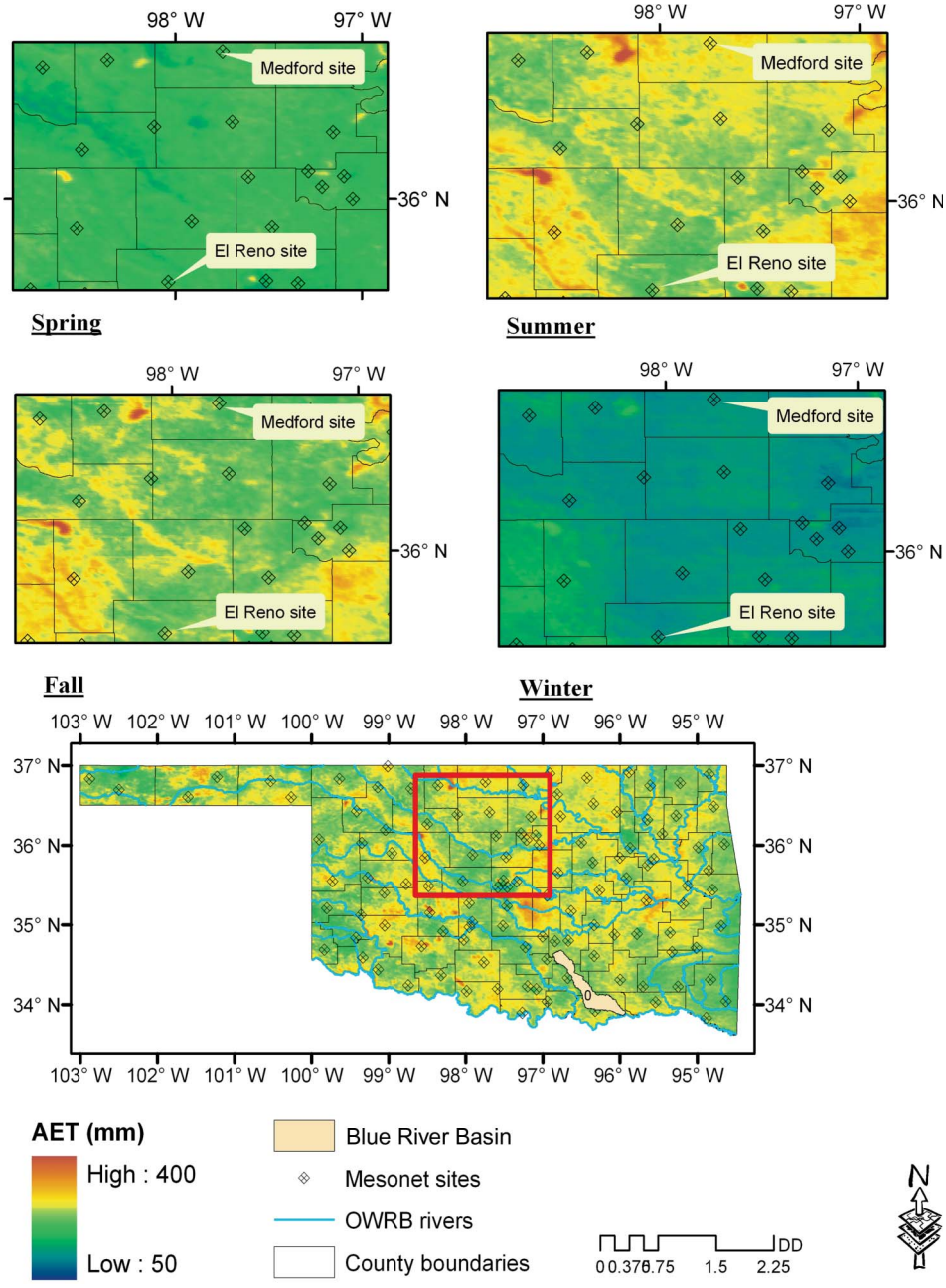

Figure 6. Seasonal actual ET in 2004 based on MM-AET with Mesonet site locations in Grant and Canadian Counties.

5. Summary and conclusion

In the past few years satellite remote sensing applications in actual ET estimation have opened frontiers in water management at local and regional scales. However, previous applications have been retrospective in nature, in part because of the lack of timely

Table 6. Data for Blue River Basin used for water balance.

Component	Data		Blue River near Connerville
Precipitation (P)	Rainfall from radar, local bias corrected	Station(s)	Radar KTLX and the following Mesonet stations: Centrahoma, Tishomingo, Sulphur, Ada, Ardmore, Lane, Madill, Newport and Pauls Valley
		Period	January–December 2005
Baseflow (G_w)	Derived from streamflow using the PART program	Station(s)	USGS 07332390
		Period	January–December 2005
Direct run-off (R)	Streamflow daily time series, baseflow removed	Station(s)	USGS 07332390
		Period	January–December 2005
Potential evapotranspiration (PET)	Monthly pan evaporation	Station(s)	Mesonet station
		Period	January–December 2005

availability of satellite images at relatively high spatiotemporal resolution. Furthermore, many ground observational networks do not provide data in real time, so that the ET estimates, though useful in retrospective studies, cannot be used in real-time water management decision making (Tang *et al.* 2009). With the availability of the world-class environmental monitoring network from Mesonet (http://mesonet.org) with 5-minute acquisition frequency, Oklahoma provides a unique setting to develop and apply a real-time ET estimation algorithm for timely water use and irrigation management. Therefore, the main objective of this paper is to assess the potentiality of implementing a real-time ET estimation algorithm by integrating satellite remote sensing and environmental monitoring network in Oklahoma, USA for operational daily water management purposes.

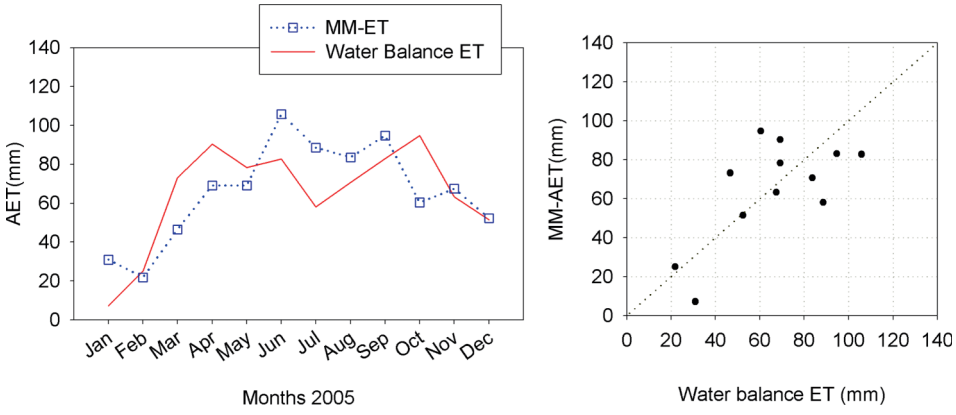

Figure 7. Comparison of the ET estimates from SEB-based MM-AET approach and water balance budget analysis for 2005 monthly average at Blue River Basin (bias ratio = 2.1%).

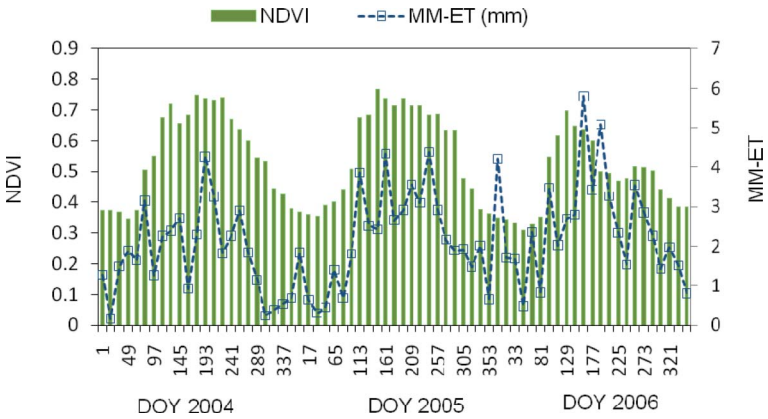

Figure 8. Temporal comparison of spatially averaged crop/vegetation index NDVI and actual ET estimates from the MM-AET approach over Blue River Basin during 2004, 2005 and 2006 (growing season typical showed high NDVI and high actual ET; also noticeable is that the dry year 2006 has less crop/vegetation but slightly higher actual ET due to sufficient supply from ground water).

In doing so, we first developed a surface-energy-balance ET estimation algorithm, MM-AET, by integrating the daily open-access MODIS products and the Oklahoma's well-distributed quality-controlled Mesonet data (5-minute acquisition frequency) through a simplified surface energy balance approach. A comprehensive evaluation of the MM-AET estimates has been conducted on daily, 8-daily, and seasonal basis for multiple years (2004–2006) using AmeriFlux tower's latent flux observations, Mesonet's *in situ* crop ET database, and water-balance-model-derived catchment-scale ET. The results show that MM-AET estimation agrees with the ground observations, with daily ET bias less than 15% and seasonal bias less than 8%. Additionally, hydrological modelled actual ET in Blue River Basin is also compared favourably with the MM-AET at catchment and monthly scale (bias ratio $< 3\%$).

Results from this study demonstrate that (1) the calculated daily ET through the developed MM-AET is acceptable for actual ET estimation given its accuracy within the range (bias $< 15\%$) reported by several studies around the world; and (2) it is feasible to implement the proposed MM-AET estimation algorithm in real time rather than in a retrospective manner for operational irrigational water resources management in Oklahoma given the twice-daily MODIS and operational surface monitoring network. This operational ET estimation system will be useful at irrigation project scales, rather than individual fields. At the time of writing, the MM-AET estimation algorithm is being implemented for the entire Oklahoma State with focus on growing season. As a natural extension, future studies include assimilating the spatially distributed ET products into a distributed hydrologic model such as *Vflo*™ (Vieux 2004) or NOAA Hydrologic Laboratory Research Distributed Hydrologic Model, for improved streamflow prediction as well as water resources management. Moreover we will focus on how to quantify water use and to determine where irrigation comprises the majority of the hydrologic water budget. The second goal is to extend and validate the remote sensing of ET in rural and urban areas under different climatic conditions and to account for irrigation water use and precipitation affecting AET.

Acknowledgements

This work was financed by the Oklahoma Water Resources Research Institute and Oklahoma Water Resource Board. Partial funding for this research is provided by NASA Earth Science Fellowship. The authors extend their appreciation to Oklahoma MESONET for providing meteorological data required for the study. We are also thankful to Professor Margaret Torn, Lawrence Berkeley, National Laboratory Earth Science, Division Berkeley, CA, for ARM SGP AmeriFlux sites data.

References

Allen, R.G., Smith, M., Perrier, A. and Pereira, L.S., 1994a, An update for the definition of reference evapotranspiration. *ICID Bulletin*, **43**, pp. 1–34.

Allen, R.G., Smith, M., Pereira, L.S. and Perrier, A., 1994b, An update for the calculation of reference evapotranspiration. *ICID Bulletin*, **43**, pp. 35–92.

Allen, R.G., Tasumi, M., Morse, A. and Trezza, R., 2005, A Landsat based energy balance and evapotranspiration model in Western US rights regulation and planning. *Irrigation and Drainage Systems*, **19**, pp. 251–268.

Allen, R.G., Tasumi, M. and Trezza, R., 2007, Satellite-based energy balance for mapping ET with internalized calibration, METRIC model. *Journal of Irrigation and Drainage Engineering*, **4**, pp. 380–394.

Baldocchi, D.D., Falge, E., Gu, L.H., Olson, R., Hollinger, D., Running, S., Anthoni, P., Bernhofer, C.H., Davis, K., Evans, R., Fuentes, J., Goldstein, A., Katul, G., Law, B., Lee, X., Malhi, Y., Meyers, T., Munger, W., Oechel, W., Paw, U.K.T., Peilgaard, K., Schmid, H.P., Valentini, R., Verma, S., Vesala, T., Wilson, K., and Wofsy, S., 2001, FLUXNET: A new tool to study the temporal and spatial variability of ecosystem-scale carbon dioxide, water vapor and energy flux densities. *Bulletin of the American Meteorological Society*, **82**, pp. 2415–2434.

Bastiaanssen, W.G.M., Menenti, M., Feddes, R.A. and Holtslang, A.A., 1998, A remote sensing surface energy balance algorithm for land (SEBAL): 1. Formulation. *The Journal of Hydrology*, **212–213**, pp. 198–212.

Bastiaanssen, W.G.M., Noordman, E.J.M., Pelgrum, H., Davids, G., Thoreson, B.P. and Allen, R.G., 2005, SEBAL model with remotely sensed data to improve water-resources management under actual field conditions. *Journal of Irrigation and Drainage Engineering*, **131**, pp. 85–93.

Bausch, W., 1995, Remote sensing of crop coefficients for improving the irrigation scheduling of corn. *Agricultural Water Management*, **27**, pp. 55–68.

Bouwer, L.M., Biggs, T.W. and Aerts, J.C.J.H., 2007, Estimates of spatial variation in evaporation using satellite-derived surface temperature and a water balance model. *Hydrological Processes*, **22**, pp. 670–682.

Brutsaert, W.H. and Sugita, M., 1992, Application of self-preservation in the diurnal evolution of the surface energy budget to determine daily evaporation. *Journal of Geophysical Research*, **97**, pp. 18377–18382.

Choudhury, B., Ahmed, N., Idso, S., Reginato, R. and Daughtry, C., 1994, Relations between evaporation coefficients and vegetation indices studied by model simulations. *Remote Sensing of Environment*, **50**, pp. 1–17.

Colditz, R.R., Conrad, C., Wehrmann, T., Schmidt, M. and Dech, S.W., 2006, Generation and assessment of MODIS time series using quality information. In *IEEE International Conference on Geoscience and Remote Sensing, IGARSS* 2006, 31 July–4 August 2006, Denver, CO, pp. 779–782.

Crago, R.D., 1996, Comparison of the evaporative fraction and the Priestley–Taylor α for parameterizing daytime evaporation. *Water Resources Research*, **32**, pp. 1403–1409.

GLENN, E.P., HUETE, A.R., NAGLER, P.L., HIRSCHBOECK, K.K. and BROWN, P., 2007, Integrating remote sensing and ground methods to estimate evapotranspiration. *Critical Reviews in Plant Sciences*, **26**, pp. 139–168.

GOWDA, P., CHAVEZ EGUEZ, J.L., COLAIZZI, P.D., EVETT, S.R., HOWELL, T.A. and TOLK, J.A. 2008, ET mapping for agricultural water management: Present status and challenges. *Irrigation Science*, **26**, pp. 223–237.

HALLDIN, S., and LINDROTH, A., 1992, Errors in net radiometry: comparison and evaluation of six radiometer designs. *Journal of Atmospheric and Oceanic Technology*, **9**, pp. 762–783.

HEILMAN, J.L. and BRITTIN, C.L., 1989, Requirements for Bowsen ratio measurements of latent and sensible heat fluxes. *Agricultural and Forest Meteorology*, **44**, pp. 261–273.

HOUBORG, R. and SOEGAARD, H., 2004, Regional simulation of ecosystem CO2 and water vapor exchange for agricultural land using NOAA AVHRR and Terra MODIS satellite data. Application to Zealand, Denmark. *Remote Sensing of Environment*, **93**, pp. 150–167.

HUETE, A., DIDAN, K., MIURA, T., RODRIGUEZ, E.P., GAO, X. and FERREIRA, L.G., 2002, Overview of the radiometric and biophysical performance of the MODIS vegetation indices. *Remote Sensing of Environment*, **83**, pp. 195–213.

HUNSAKER, D., PINTER, P., BARNES, E. and KIMBALL, B., 2003, Estimating cotton evapotranspiration crop coefficients with a multispectral vegetation index. *Irrigation Science*, **22**, pp. 95–104.

HUNSAKER, D., PINTER, P. and KIMBALL, B. 2005, Wheat basal crop coefficients determined by normalized difference vegetation index. *Irrigation Science*, **24**, pp. 1–14.

HUNTINGTON, T., 2006, Evidence for intensification of the global water cycle: review and synthesis. *Journal of Hydrology*, **319**, pp. 83–95.

HUXMAN, T., WILCOX, B., BRESHEARS, D., SCOTT, R., SNYDER, K., SMALL, E., HULTINE, K., POCKMAN, W. and JACKSON, R., 2005, Ecohydrological implications of woody plant encroachment. *Ecology*, **86**, pp. 308–319.

IRMAK, A. and IRMAK, S., 2008, Reference and crop evapotranspiration in south central Nebraska. II: Measurement and estimation of actual evapotranspiration. *Journal of Irrigation and Drainage Engineering*, **134**, pp. 700–715.

JACKSON, R., 1986, Estimating aerial evapotranspiration by combining remote sensing and ground-based data. In *Remote Sensing Applications for Consumptive Use (Evapotranspiration), American Water Resources Association Monograph Series No. 6*, A. Johnson and A. Rango (Eds), pp. 13–24 (Bethesda, Maryland: IAHS Publications).

JIANG, H., LIU, S., SUN, P., AN, S., ZHOU, G., LI, C., WANG, J., YU, H. and TIAN, X., 2004, The influence of vegetation type on the hydrological process at the landscape scale. *Canadian Journal of Remote Sensing*, **30**, pp. 743–763.

JIANG, L. and ISLAM, S., 2001, Estimation of surface evaporation map over southern Great Plains using remote sensing data. *Water Resources Research*, **37**, pp. 329–340.

JIN, Y., SCHAAF, C.B., GAO, F., LI, X. and STRAHLER, A.H., 2003, Consistency of MODIS surface BRDF/albedo retrievals: 1. Algorithm performance. *Journal of Geophysical Research*, **108**, p. 4158.

JUSTICE, C.O., TOWNSHEND, J.R.G., VERMOTE, E.F.E., MASUOKA, R.E., WOLFE, N.Z., EL SALEOUS, D.P., and MORISETTE, J.T., 2002, An overview of MODIS land data processing and product status. *Remote Sensing of Environment*, **83**, pp. 3–15.

KALMA, J.D., MCVICAR, T.R. and MCCABE, M.F., 2008, Estimating land surface evaporation: A review of methods using remotely sensing surface temperature data. *Surveys in Geophysics*, **29**, pp. 421–469.

KITE, G.W. and PIETRONIRO, A., 1996, Remote sensing applications in hydrological modeling. *Hydrological Sciences Journal*, **41**, pp. 563–592.

KUITTINEN, R., 1992, Remote sensing for hydrology progress and prospects, WMO Operational Hydrology Report, No. 36, WMO-No. 773, Geneva, Switzerland.

Lewis, J.M., 1995, The story behind the Bowen ratio. *Bulletin of the American Meteorological Society*, **76**, pp. 2433–2443.

McPherson, R.A., Fiebrich, C.A., Crawford, K.C., Kilby, J.R., Grimsley, D.L., Martinez, J.E., Basara, J.B., Illston, B.G., Morris, D.A., Kloesel, K.A., Melvin, A.D., Shrivastava, H., Wolfinbarger, J.M., Bostic, J.P., Demko, D.B., Elliott, R.L., Stadler, S.J., Carlson, J.D. and Sutherland, A.J., 2007, Statewide monitoring of the mesoscale environment: A technical update on the Oklahoma Mesonet. *Journal of Atmospheric and Oceanic Technology*, **24**, pp. 301–321.

Meehl, G.A., Stocker, T.F., Collins, W.D., Friedlingstein, P., Gaye, A.T., Gregory, J.M., Kitoh, A., Knutti, R., Murphy, J.M., Noda, A., Raper, S.C.B., Watterson, I.G., Weaver, A.J. and Zhao, Z.C., 2007, Global climate projections. In *Climate Change 2007: The Physical Science Basis. Contribution of Working Group I to the Fourth Assessment Report of the Intergovernmental Panel on Climate Change*, S. Solomon, D. Qin, M. Manning, Z. Chen, M. Marquis, K.B. Averyt, M. Tignor and H.L. Miller (Eds), p.238 (Cambridge, UK and New York, NY: Cambridge University Press).

Mu, Q., Heinsch, F.A., Zhao, M. and Running, S.W., 2007, Development of a global evapotranspiration algorithm based on MODIS and global meteorology data. *Remote Sensing of Environment*, **111**, pp. 519–536.

Nagler, P., Cleverly, J., Lampkin, D., Glenn, E., Huete, A. and Wan, Z. 2005, Predicting riparian evapotranspiration from MODIS vegetation indices and meteorological data. *Remote Sensing of Environment*, **94**, pp. 17–30.

Nishida, K., Nemani, R.R., Running, S.W. and Glassy, J.M., 2003, An operational remote sensing algorithm of land surface evaporation. *Journal of Geophysical Research*, **108**, 4270.

Norman, J., Anderson, M., Kustas, W., French, A., Mecikalski, J., Torn, R., Diak, G., Schmugge, T. and Tanner, B., 2003, Remote sensing of surface energy fluxes at 101-m pixel resolutions. *Water Recourses Research*, **39**, pp. 1221.

Rango, A. and Shalaby, A.I., 1998, Operational applications of remote sensing in hydrology: success, prospects and problems. *Hydrological Sciences Journal*, **43**, pp. 947–968.

Santanello, J.A., Lidard, C.D., Garcia, M.E., Mocko, D.M., Tischler, M.A.M. and Moranthoma, D.P., 2007, Using remotely-sensed estimates of soil moisture to infer soil texture and hydraulic properties across a semi-arid watershed. *Remote Sensing of Environment*, **110**, pp. 79–97.

Schaaf, C., Gao, F., Strahler, A., Lucht, W., Li, X., Tsang, T., Strugnell, N., Zhang, X., Jin, Y. and Muller, J., 2002, First operational BRDF, albedo and nadir reflectance products from MODIS. *Remote Sensing of Environment*, **83**, pp.135–148.

Seevers, P. and Ottomann, R., 1994, Evapotranspiration estimation using a normalized difference vegetation index transformation of satellite data. *Hydrological Sciences Journal*, **39**, pp. 333–345.

Seguin, B., Courault, D. and Guérif, M., 1994, Surface temperature and evapotranspiration: Application of local scale methods to regional scales using satellite data. *Remote Sensing of Environment*, **49**, pp. 287–295.

Senay, G.B., Budde, M., Verdin, J.P. and Melesse, A.M., 2007. A coupled remote sensing and simplified surface energy balance approach to estimate actual evapotranspiration from irrigated fields. *Sensors*, **6**, pp. 979–1000.

Shiklomanov, I.A., 1998, *World Water Resources: A New Appraisal and Assessment for the 21st Century* (Paris: UNESCO).

Shuttleworth, W.J., 1991, Insight from large-scale observational studies of land/atmosphere interactions. *Surveys in Geophysics*, **12**, pp. 3–30.

Shuttleworth, W.J., Gurney, R.J., Hsu, A.Y. and Ormsby, J.P., 1989, FIFE: The variation in energy partition at surface flux sites. In *Remote Sensing and Large-Scale Processes,*

Proceedings of the IAHS Third International Assembly, A. Rango (Ed.), 14 August 1989 Baltimore, MD, pp. 67–74 (Baltimore, MD: IAHS Publications).

SOBRINO, J.A., GÓMEZ, M., JIMÉNEZ-MUÑOZ, J.C., OLIOSO, A., 2007, Application of a simple algorithm to estimate the daily evapotranspiration from NOAA-AVHRR images for the Iberian Peninsula. *Remote Sensing of Environment*, **110**, pp. 139–148.

STEWART, J.B, WATTS, C.J., RODRIGUEZ, J.C., DE BRUIN, H.A.R., VAN DEN BERG, A.R. and GARATUZ-PAYAN, J., 1999, Use of satellite data to estimate radiation and evaporation for northwest Mexico. *Agricultural Water Management*, **38**, pp. 181–193.

SU, B., 2002, The surface energy balance system (SEBS) for the estimation of turbulent heat fluxes. *Hydrology and Earth System Sciences*, **6**, pp. 85–99.

SUGITA, M. and BRUTSAERT, W., 1991, Daily evaporation over a region from lower boundary layer profiles measured with radiosondes. *Water Resources Research*, **27**, pp. 747–752.

SZILAGYI, J., 2000, Can a vegetation index derived from remote sensing be indicative of areal transpiration? *Ecological Modeling*, **127**, pp. 65–79.

SZILAGYI, J., 2002, Vegetation indices to aid areal evapotranspiration estimations. *Journal of Hydrologic Engineering*, **7**, pp. 368–372.

TANG, Q., PETERSON, S., CUENCA, R.H., HAGIMOTO, Y. and LETTENMAIER, D.P., 2009, Satellite-based near-real-time estimation of irrigated crop water consumption. *Journal of Geophysical Research*, **114**, p. 5114.

TASUMI, M., TREZZA, R., ALLEN, R. and WRIGHT, J., 2005, Operational aspects of satellite-based energy balance models for irrigated crops in the semi-arid U.S. *Irrigation and Drainage Systems*, **19**, pp. 355–376.

VENTURINI, V., ISLAM, S. and RODRIGUEZ, L., 2008, Estimation of evaporative fraction and evapotranspiration from MODIS products using a complementary based model. *Remote Sensing of Environment*, **112**, pp. 132–141.

VERMOTE, E.F., TANRE, D., DEUZE, J.L., HERMAN, M., and MORCRETTE, J.J., 1997, Second simulation of the satellite signal in the solar spectrum: An overview. *IEEE Transactions on Geoscience and Remote Sensing*, **35**, pp. 675–686.

VIEUX, B.E., 2004, *Distributed Hydrologic Modeling Using GIS*, 2nd edn, (Norwell, MA: Kluwer Academic Publishers). Water Science Technology Series, Vol. 48. CD-ROM including model software and documentation.

WAN, Z-M., and LI, Z.-L., 1997, A physics-based algoritum for retrieving land surface emissivity and temperature from EOS/MODIS data. *IEEE Transactions on Geoscience and Remote Sensing*, **35**, pp. 980–996.

WAN, Z., ZHANG, Y., ZHANG, Q. and LI, Z.L., 2004, Quality assessment and validation of the MODIS global land surface temperature, *International Journal of Remote Sensing*, **25**, pp. 261–271.

WANG, K., WANG, P., LI, Z., SPARROW, M. and CRIBB, M., 2007, A simple method to estimate evapotranspiration from a combination of net radiation, vegetation indices and temperatures. *Journal of Geophysical Research*, **112**, D15107, doi: 10.1029/2006JD008351.

WRIGHT, J.L., 1996, Derivation of alfalfa and grass reference evapotranspiration. Evapotranspiration and irrigation scheduling. In *Proceedings of the International Conference, ASAE*, C.R. Camp, E.J. Sadler and R.E. Yoder (Eds), 3–6 November 1996, San Antonio, TX, pp. 133–140.

ZHAO, M., HEINSCH, F.A., NEMANI, R. and RUNNING, S.W., 2005, Improvements of the MODIS terrestrial gross and net primary production global data set. *Remote Sensing of Environment*, **95**, pp. 164–176.